

Density peaking and turbulent pinch in DIII-D discharges

C. Estrada-Mila

Department of Mechanical and Aerospace Engineering, University of California San Diego, La Jolla, California 92093

J. Candy and R. E. Waltz

General Atomics, San Diego, California 92121

(Received 11 May 2006; accepted 28 June 2006; published online 24 July 2006)

A study of density peaking and particle flow in low confinement (L-mode) DIII-D discharges [G. R. McKee, C. C. Petty, R. E. Waltz *et al.*, Nucl. Fusion **41**, 1235 (2001)], using global gyrokinetic simulations, is presented. It is found that under experimental conditions, in particular when realistic collisionality is included, a turbulent pinch driven by electron temperature and density gradients can occur. © 2006 American Institute of Physics. [DOI: 10.1063/1.2241767]

Density peaking has recently attracted considerable experimental^{1–5} and theoretical modelling^{1,6–9} attention. Its importance relies on the fact that a peaked profile can increase the power production, energy confinement, and bootstrap current of the plasma. On the other hand, an excessively peaked pressure profile can reduce the stability limit. For these reasons, it is important to understand this phenomenon, and predict its occurrence and effects in future reactors such as ITER.¹⁰ Evidence found in low confinement (L-mode) discharges^{11,12} suggests that a turbulent particle pinch (flow against density gradients) is responsible for the observed peaking. Another candidate, the neoclassical Ware pinch,¹³ is usually too small to explain experimental observations. Large tokamaks like DIII-D have very weak plasma flows as a consequence of almost negligible particle sources in the core. However, by looking at the observed peaked density profiles one would expect the density gradients to drive a significant outward flow. This apparent contradiction is usually resolved by taking into account some inward flow or pinch to nearly cancel the outflow and yield the experimental levels. In more detail, if we write the total or net electron particle flux as a sum of diffusive and convective contributions we get

$$\Gamma_e \doteq -D_e^d \frac{\partial n_e}{\partial r} - n_e v_{in}, \quad (1)$$

where D_e^d is the turbulent diffusion coefficient and v_{in} is an inward convective (i.e., pinch) velocity. Consequently, in order to get $\Gamma_e \rightarrow 0$ and keep the density profile from flattening, the pinch term must balance the diffusive term.

From a theoretical point of view, two different mechanisms have been proposed as being responsible for such anomalous pinch. The first one, usually called thermodiffusion, was first developed in the collisional regime¹⁴ and subsequently extended to the dissipative (low collisionality) regime.¹⁵ Thermodiffusion predicts an inward flow component of the total transport proportional to $\nabla T_e / T_e$, where T_e is the electron temperature. The second mechanism, sometimes called turbulent equipartition,^{16–19} involves the magnetic field curvature and can induce a pinch as the result of subtle functional constraints. Recent numerical studies of ion tem-

perature gradient (ITG) and trapped electron mode (TEM) turbulence, have devoted attention to this problem using fluid²⁰ and gyrokinetic simulations.²¹ These works found enough evidence of a turbulent pinch for typical experimental parameters, but despite these advances, the connection between density peaking and said pinch remains unclear. One of the main reasons is that density peaking is a global problem, whereas previous studies were either highly realistic but local,²¹ or global²⁰ but with simplified physics. Another problematic issue with ITG/TEM simulations is the strong reduction of the pinch intensity when realistic collisionality is included.^{6,21}

The purpose of this Brief Communication is to answer, via gyrokinetic simulations, if the ITG/TEM pinch can be responsible for the observed density peaking in experiments. This question was previously addressed using linear gyrokinetic simulations and a quasilinear model.⁹ It was found that for the most relevant cases such a description failed to describe the peaking. However, we believe that the main issue is not a question of the physics model involved but of the realism of the simulations used. To test this hypothesis we present GYRO (Ref. 22) simulations of a DIII-D L-mode discharge (shot 101391).²³ In GYRO, only perturbations or deviations from a given equilibrium are evolved, whereas equilibrium profiles are kept fixed. The simulations presented here include nonlinear gyrokinetic ions and electrons, radial profile variation with $\mathbf{E} \times \mathbf{B}$ rotation, shaped geometry, electron pitch-angle scattering and electromagnetic fluctuations. Previous studies²⁴ have shown that this level of realism is enough to match the experimentally inferred energy transport coefficients with less than 10% adjustment of the ion temperature gradient. It is important to emphasize that this work should be seen as a numerical exercise, in which we are trying to reconcile simulations with experimental observations, rather than a direct comparison between fluxes.

In the simulations that follow, length is measured in units of the minor radius a , mass in units of the ion mass m_i , temperatures in units of T_e (electron temperature), and velocities in units of the ion sound speed ($c_s \doteq \sqrt{T_e / m_i}$). Frequencies and growth rates use a combination of the former and are measured in units of c_s / a . Diffusivities are normal-

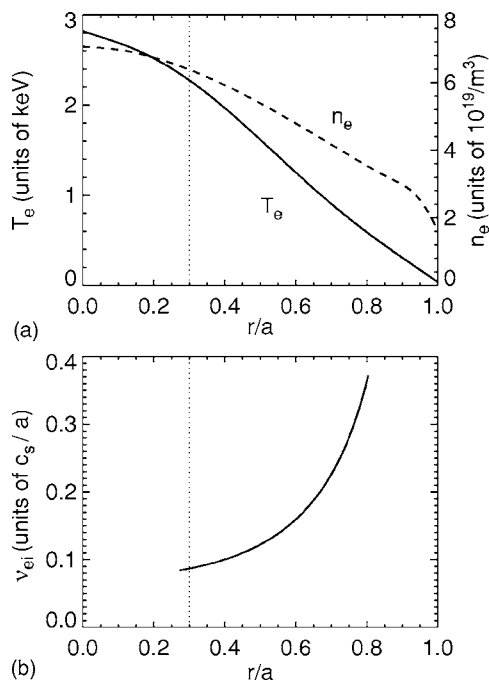


FIG. 1. DIII-D profile data for discharge 101391. Plot (a) shows experimental electron density and temperature profiles, while plot (b) shows the calculated electron-ion collisionality based on these profiles. The vertical dotted lines denote the radial domain used in the simulations.

ized to a reference gyro-Bohm level $\chi_{GB} \doteq \rho_s^2 c_s / a$, where $\rho_s \doteq c_s / \Omega_{ci}$ is the ion-sound Larmor radius and $\Omega_{ci} = eB/m_i$ is the ion cyclotron frequency. In these units the relative gyro-radius can be written as $\rho^* \doteq \rho_s / a$. It is important to mention that all of the simulations used in this study have the same reference radius ($r/a=0.6$). The reference radius is the point where normalizations such as c_s or ρ_s are computed and where the resolution is best. For example, at this radius the electron-ion collision frequency is given by $\nu_{ei}=0.16$ (units of c_s/a) and $\rho^*=0.0025$. A detailed summary of all the experimental parameters with their respective physical units is given in Ref. 25, Table I, and some of the most relevant experimental profiles are shown in Fig. 1. Finally, these simulations include two gyrokinetic species (ions and electrons), and equal density gradients ($1/L_{ni}=1/L_{ne}$) to satisfy plasma neutrality. In this work, as well as in our previous one,²¹ we consider only electron-ion pitch-angle collisions, where ν_{ei} is taken from experiments. The details of the collision operator can be found in Ref. 22.

With respect to code resolution we use a 128-point velocity-space grid (8 energies, 8 pitch angles, and 2 signs of velocity), and 10 poloidal (orbit) grid points per sign of velocity. For the radial direction we employ a nonuniform grid with 360 radial grid points and a span of $0.3 < r/a < 0.8$. Finally, in the k_θ direction we have $n_n=16$ complex toroidal modes and resolve up to $k_{\theta\rho_s} \leq 0.9$. This resolution is almost identical to that used in Ref. 25, although the radial resolution is 50% higher (360 instead of 240 radial grid points). It is important to mention that we used a reduced ion to electron mass ratio ($\mu_e \doteq \sqrt{m_i/m_e}$) of 40 instead of the physical 60, which is computationally more efficient, and does not significantly alter the results. Indeed, a previous study,²⁵

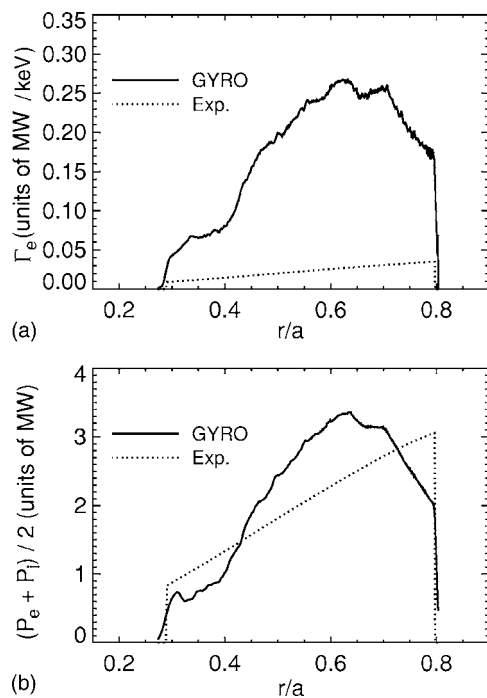


FIG. 2. Radial electron particle flow in MW/keV (a) and average energy flow in MW (b) from the baseline simulation (solid line) compared to their experimental counterparts.

found that $\mu_e=40$ (even $\mu_e=30$) is more than adequate for this type of discharge. Since these simulations include profile variation, an adaptive source is used to avoid profile gradient relaxation and ensure that there is no turbulent modification to the equilibrium density and temperature profiles. It is important to clarify that the numerical sources will match the experimental ones if the simulated power profiles match perfectly. The details of the algorithm used can be found in Ref. 26.

The strategy used in this study was to initially obtain a baseline case that matches the experiment, and subsequently change the electron density $\{L_{ne} \doteq -[\partial(\ln n_e)/\partial r]^{-1}\}$ and temperature $\{L_{Te} \doteq -[\partial(\ln T_e)/\partial r]^{-1}\}$ gradient lengths to determine the pinch term effects and their relevance under experimental conditions. The resulting electron particle flow for the baseline case compared to the experimental one is shown in Fig. 2(a), and the resulting average energy flow $(P_e + P_i)/2$ is shown in Fig. 2(b). Notice that in this, and all other simulations, we smoothed the plots with a 5-point boxcar average to guide the eye. We also lowered $1/L_{Ti}$ by 10% in all our cases in order to match the experimental χ_i and χ_e , otherwise the levels predicted could be a factor of 2 higher than the experimental ones. This strong sensitivity of χ_i and χ_e to L_{Ti} is a consequence of the stiffness inherent in the transport problem, which is rather striking if we consider that the experimental error for $1/L_{Ti}$ is about 10% as well. To further highlight the difficulty of this problem, the averaged experimental electron and ion power at $r/a=0.6$ and $T_e=1.25$ keV is 2.28 MW, whereas the experimental electron plasma flow is only 0.0256 MW/keV at the same radius and temperature. We emphasize that the small value of the electron plasma flow, which is the result of an almost negli-

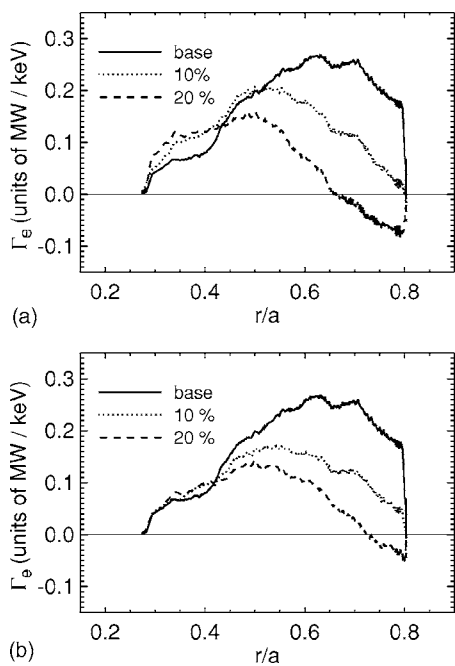


FIG. 3. Plot (a) shows the variation of radial electron particle flow as $1/L_{Te}$ is increased by 10% and 20% while $1/L_{ne}$ is kept fixed. Plot (b) shows the same variation when $1/L_{Te}$ is decreased by 10% and 20% and $1/L_{ne}$ is kept fixed.

gible particle source, is very difficult to replicate in the simulations without adjusting the electron profiles. However, the average energy flow [Fig. 2(b)] shows very good agreement between simulation and experiment showing that the relevant physics is captured overall.

For the first scan we kept $1/L_{ne}$ fixed to its experimental value and raised $1/L_{Te}$ by 10% and 20%. The resulting plasma flow can be seen in Fig. 3(a). Increasing the electron temperature gradient reduces the flow magnitude for both cases as expected from ITG considerations, and in the 20% case it creates a negative net flow ($\Gamma_e < 0$) for $r/a > 0.65$. A similar effect, albeit less dramatic, can be observed in Fig. 3(b) when $1/L_{Te}$ is decreased by 10% and 20%, while keeping $1/L_{ne}$ fixed to its experimental value. In this case the pinch term is not as strong, although the net flow is considerably reduced in most of its radial domain. It is important to mention that the experimental error for $1/L_{Te}$ and $1/L_{ne}$ is around 5% and 10%, respectively. For the final scan we used a combination of the former, and simultaneously raised and decreased $1/L_{Te}$ and $1/L_{ne}$, respectively, as shown in Fig. 4. Unsurprisingly, the most dramatic effects are observed in this case, where the total flow is greatly reduced for the 10% case with $\Gamma_e < 0$ in some regions ($r/a > 0.7$), and strongly negative for $r/a > 0.55$ in the 20% case.

One might object to these results on the grounds that they were obtained by adjusting the gradients everywhere by the same amount, or that the 20% cases were above the experimental uncertainty. However, our main objective was to illustrate the possibility of obtaining a pinch and consequently a density peaking under experimental conditions, in particular when “high” collisionality is included. An improvement over this work can be done by adjusting individu-

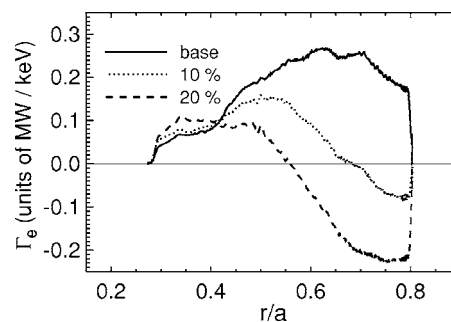


FIG. 4. Variation of radial electron particle flow as $1/L_{Te}$ is increased and $1/L_{ne}$ is decreased simultaneously by 10% and 20%.

ally the temperature and/or density gradients using a feedback mechanism, in order to get a “perfect” matching with the experimental flows. This type of approach, which has been used successfully in a simpler electrostatic simulation with $\mu_e = 20$ and $\rho_* = 0.004$,²⁷ found that when the simulation flows agrees with the experimental ones at every radius, a peaking of the density is observed. The discharge in Ref. 27 is dimensionally similar to the discharge considered here and therefore has the same collisionality.

To summarize this work, we simulated L-mode DIII-D discharges using gyrokinetic simulations of ITG/TEM turbulence and found the existence of a pinch under experimental conditions, reconciling the apparent discrepancies between anomalous pinches and collisionality. This evidence supports our hypothesis that fully realistic simulations are crucial to the reliable calculation of experimental flows.

This work was supported by the U.S. Department of Energy Grant No. DE-FG03-95ER54309.

- ¹C. Angioni, A. G. Peeters, X. Garbet, A. Manini, F. Ryter, and ASDEX Upgrade Team, Nucl. Fusion **44**, 827 (2004).
- ²M. Valovic, R. Budny, L. Garzotti, X. Garbet, A. A. Korotkov, J. Rapp, R. Neu, O. Sauter, P. deVries, B. Alper, M. Beurskens, J. Brzozowski, D. McDonald, H. Leggate, C. Giroud, V. Parail, I. Voitsekhovitch, and JET EFDA contributors, Plasma Phys. Controlled Fusion **46**, 1877 (2004).
- ³M. Romanelli, C. Bourdelle, and W. Dorland, Phys. Plasmas **11**, 3845 (2004).
- ⁴H. Weisen, A. Zabolotsky, C. Angioni, I. Furno, X. Garbet, C. Giroud, H. Leggate, P. Mantica, D. Mazon, J. Weiland, L. Zabeo, K.-D. Zastrow, and JET-EFDA contributors, Nucl. Fusion **4**, 5 (2005).
- ⁵A. Zabolotsky, H. Weisen, and TCv Team, Plasma Phys. Controlled Fusion **48**, 369 (2006).
- ⁶C. Angioni, A. G. Peeters, G. V. Pereverzev, F. Ryter, G. Tardini, and ASDEX Upgrade Team, Phys. Plasmas **10**, 3225 (2003).
- ⁷G. V. Pereverzev, C. Angioni, A. G. Peeters, and O. V. Zolotukhin, Nucl. Fusion **45**, 221 (2005).
- ⁸A. G. Peeters, C. Angioni, M. Apostoliceanu, G. V. Pereverzev, E. Quigley, F. Ryter, D. Strintzi, F. Jenko, U. Fahrbach, C. Fuchs, O. Gehre, J. Hobirk, B. Kurzan, C. F. Maggi, A. Manini, P. J. McCarthy, H. Meister, J. Schweinzer, J. Stober, W. Suttrop, G. Tardini, and the ASDEX Upgrade Team, Nucl. Fusion **45**, 1140 (2005).
- ⁹C. Angioni, A. G. Peeters, F. Jenko, and T. Dannert, Phys. Plasmas **12**, 112310 (2005).
- ¹⁰ITER Physics Basis Editors, Nucl. Fusion **39**, 2175 (1999).
- ¹¹A. Zabolotsky, H. Weisen, and TCv Team, Plasma Phys. Controlled Fusion **45**, 735 (2003).
- ¹²L. Garzotti, X. Garbet, P. Mantica, V. Parail, M. Valovic, G. Corrigan, D. Heading, T. T. C. Jones, P. Lang, H. Nordman, B. Pégourié, G. Saibene, J. Spence, P. Strand, J. Weiland, and contributors to the EFDA-JET Workprogramme, Nucl. Fusion **43**, 1829 (2003).
- ¹³A. A. Ware, Phys. Rev. Lett. **25**, 15 (1970).

- ¹⁴B. Coppi and C. Spight, *Phys. Rev. Lett.* **41**, 551 (1978).
- ¹⁵R. E. Waltz and R. R. Dominguez, *Phys. Fluids B* **1**, 1935 (1989).
- ¹⁶V. V. Yancov, *JETP Lett.* **60**, 171 (1994).
- ¹⁷M. B. Isichenko, A. V. Gruzinov, and P. H. Diamond, *Phys. Rev. Lett.* **74**, 4436 (1995).
- ¹⁸D. R. Baker and M. N. Rosenbluth, *Phys. Plasmas* **5**, 2936 (1998).
- ¹⁹D. R. Baker, *Phys. Plasmas* **11**, 992 (2004).
- ²⁰X. Garbet, L. Garzotti, P. Mantica, H. Nordman, M. Valovic, H. Weisen, and C. Angioni, *Phys. Rev. Lett.* **91**, 035001 (2001).
- ²¹C. Estrada-Mila, J. Candy, and R. E. Waltz, *Phys. Plasmas* **12**, 022305 (2005).
- ²²J. Candy and R. E. Waltz, *J. Comput. Phys.* **186**, 545 (2003).
- ²³G. R. McKee, C. C. Petty, R. E. Waltz, C. Fenzi, R. J. Fonck, J. E. Kinsey, T. C. Luce, K. H. Burrell, D. R. Baker, E. J. Doyle, X. Garbet, R. A. Moyer, C. L. Rettig, T. L. Rhodes, D. W. Ross, G. M. Staebler, R. Sydora, and M. R. Wade, *Nucl. Fusion* **41**, 1235 (2001).
- ²⁴J. Candy and R. E. Waltz, *Phys. Rev. Lett.* **91**, 045001 (2003).
- ²⁵R. E. Waltz, J. Candy, and C. C. Petty, *Phys. Plasmas* **13**, 072304 (2006).
- ²⁶R. E. Waltz, J. Candy, F. L. Hinton, C. Estrada-Mila, and J. E. Kinsey, *Nucl. Fusion* **45**, 741 (2005).
- ²⁷R. E. Waltz, *Fusion Sci. Technol.* **48**, 1051 (2005).